[82] A. Avsar, T.-Y. Yang, S. Bae, *et al.* 'Toward Wafer Scale Fabrication of Graphene Based Spin Valve Devices'. *Nano Lett.* **11**, 2363 (2011).

[83] B. Birkner, D. Pachniowski, A. Sandner, *et al.* 'Annealing-induced magnetic moments detected by spin precession measurements in epitaxial graphene on SiC'. *Phys. Rev. B* **87**, 081405 (2013).

[84] H. Idzuchi, A. Fert, and Y. Otani. 'Revisiting the measurement of the spin relaxation time in graphene-based devices'. *Phys. Rev. B* **91**, 241407 (2015).

Chapter 3

Thermal and thermoelectric transport in graphene

Abstract

This chapter consists of two sections. The first section explains the basics of thermoelectrics in metals, by considering the Seebeck and Peltier effect, and their reciprocity. The second section starts with a description of the thermal transport properties of graphene by focusing on their underlying physical origins, followed by a description of recent developments in graphene thermoelectric experiments. The latter discussion concentrates mostly on showing the workings and achievements of the experimental methods that are used to study graphene's special thermoelectric behavior.

A temperature gradient in a material can be created by connecting it to two thermal reservoirs with $T_1 > T_2$ as depicted in Figure 3.1(a). The gradient gives rise to a steady-state heat current towards the low temperature side, as described by Fourier's law (in the one-dimensional case):

$$j_Q = -\kappa \frac{\mathrm{d}T}{\mathrm{d}x}. \tag{3.1}$$

Here, j_Q is the heat current density, κ is the thermal conductivity and T the temperature. In metals, heat is carried mostly by the conduction electrons. The notion that electrons are the primary carriers for kinetic energy (heat) is reflected in the Wiedemann–Franz law,[1] which states that the ratio of the thermal conductivity and the electrical conductivity σ in a metal is constant. The temperature dependence of this constant is given by:

$$\frac{\kappa}{\sigma} = LT. \tag{3.2}$$

Here, L is the Lorentz number[2] given by $L = \frac{\pi^2}{3}\left(\frac{k_B}{e}\right)^2 = 2.45 \times 10^{-8}$ W Ω K^{-1}.From the simple fact that electrons are affected by both temperature and voltage gradients, one can expect that cross links exists between heat and charge transport. This is the field of *thermoelectrics*. In the following section a number of thermoelectric effects will be treated.

3.1 Thermoelectric effects

Onsager reciprocity Two flows or currents $\vec{j_1}$ and $\vec{j_2}$ (e.g. a heat and a charge current) are related to the respective thermodynamic forces that drive these currents $\vec{X_1}$

and $\vec{X}_2$ (e.g. an electromotive force and a temperature gradient) by the relationship:

$$\begin{pmatrix} \vec{j}_1 \\ \vec{j}_2 \end{pmatrix} = \begin{pmatrix} L_{11} & L_{12} \\ L_{21} & L_{22} \end{pmatrix} \begin{pmatrix} \vec{X}_1 \\ \vec{X}_2 \end{pmatrix} \tag{3.3}$$

This relationship describes any system where two transport processes are happening simultaneously. Each coefficient L_{ij} can be understood as the specific conductance for the related transport process. For $i \neq j$, the coefficient relates the interdependency of these two transport processes.

Onsager showed that, when the system is close to equilibrium, the relationship

$$L_{12} = L_{21} \tag{3.4}$$

holds.[3] This thermodynamic relationship is called *Onsager reciprocity*.[a]

When considering charge and heat flows specifically, equation 3.3 becomes (in the one-dimensional case):

$$\begin{pmatrix} j \\ j_\mathrm{Q} \end{pmatrix} = -\begin{pmatrix} \sigma & \sigma S \\ \sigma\Pi & \kappa \end{pmatrix} \begin{pmatrix} \frac{\mathrm{d}V}{\mathrm{d}x} \\ \frac{\mathrm{d}T}{\mathrm{d}x} \end{pmatrix} \tag{3.5}$$

This expression includes Ohm's law (equation 2.1), Fourier's law (equation 3.1) and two other laws that describe the interdependency of charge and heat transport: the *Seebeck effect* and the *Peltier effect*. S and Π are called the Seebeck coefficient and the Peltier coefficient.

The Seebeck effect When a temperature difference ΔT exists between two ends of a material, a potential difference ΔV is created:

$$\Delta V = S\Delta T \tag{3.6}$$

The strength of this effect is given by the Seebeck coefficient or thermopower S, which is a material specific property. The sign of S is defined in such a way, that the temperature gradient points in the opposite direction as the voltage gradient. For metals, where electronic transport takes place at the Fermi energy E_F, S can be related to the conductivity σ by the Mott relation:[4, 5]

$$S = -\frac{\pi^2 k_\mathrm{B}^2 T}{3|e|} \frac{\mathrm{d}\ln\sigma(E)}{\mathrm{d}E}\bigg|_{E=E_\mathrm{F}}. \tag{3.7}$$

Figure 3.1 shows how a heat current between two thermal reservoirs can be accompanied by a charge current. At finite temperatures, the density of states $\nu(E) \propto \sqrt{E}$

[a] In his paper, Onsager describes the condition of local thermal equilibrium with the term microscopic reversibility. This means that any fluctuation in the system state or configuration is balanced out, because it is as likely to occur as its time-reverse. Onsager showed that equation 3.4 holds using only this condition, regardless of the mechanism causing such a fluctuation.

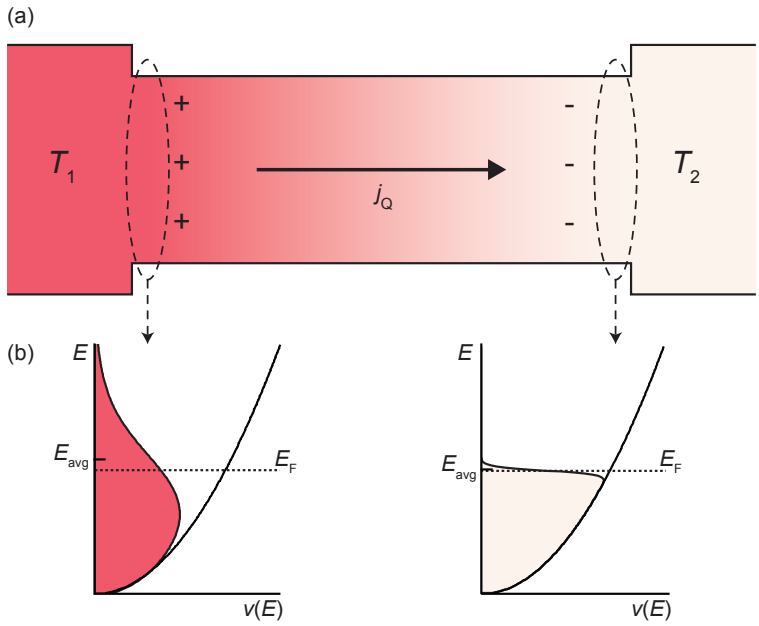

Figure 3.1: Depiction of the Seebeck effect. (a) A thermal gradient drives a heat current j_Q through a channel between two thermal reservoirs with $T_1 > T_2$. If the material has a finite Seebeck coefficient, this leads to an internal Seebeck voltage. (b) The heat current originates from the fact that the thermalized heat carriers (here electrons) on the hot side (left) of the channel have on average a higher energy E_{avg} than on the cold side (right). Through diffusion, a steady-state heat current flows from hot to cold. Because the electrical conductivity depends on the energy, carriers on one side are transported more effectively than on the other, thus building up a Seebeck voltage.

in the heat channel broadens, by multiplication with the Fermi–Dirac distribution $f(E) = [\exp\left(\frac{E-E_{\mathrm{F}}}{k_{\mathrm{B}}T}\right) + 1]^{-1}$ (Figure 3.1(b)). The Seebeck effects arises because the electrical conductivity $\sigma(E)$ depends on the diffusion coefficient and thus on the energy. This means that electrons on one side of the channel will be transported more effectively than on the other side, resulting in a net flow of charge. In steady-state conditions, the charge accumulation leads to an internal voltage build-up. Consequently, if for a material the conductivity is strongly dependent on the energy (reflected in a high energy derivative), the magnitude of S is high.

When sending a heat current through an interface between two materials with different Seebeck coefficients $S_1 \neq S_2$, a voltage develops over its interface, as depicted in Figure 3.2(a). The measured voltage is given by $V = \Delta V_1 - \Delta V_2 = (S_1 - S_2)\Delta T$. This is the underlying principle of a thermocouple, which is basically the use of an interface between two different Seebeck materials as a thermometer. The output volt-

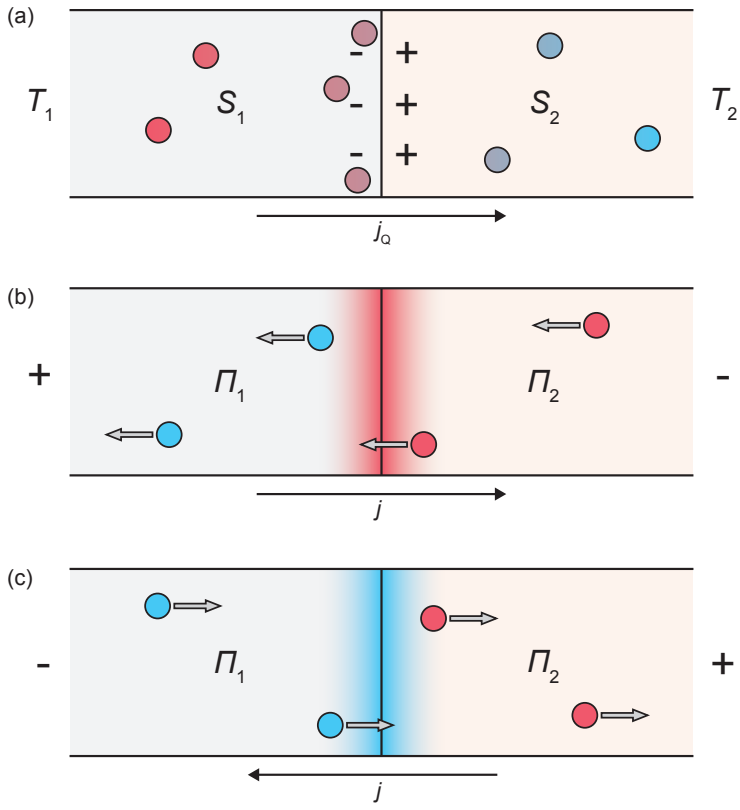

Figure 3.2: (a) If a heat current flows across the interface between two materials with different Seebeck coefficients $S_1 \neq S_2$, transport of the carriers (here electrons) in one direction is favored over the other, leading to an accumulation of charge. This is because at a given T, the materials have a different number of thermalized states available for transport. This principle is exploited in thermocouples, where the voltage that develops can be used to extract information about the local temperature. (b)-(c) If a charge current is sent across the interface between two materials with different Peltier coefficients $\Pi_1 \neq \Pi_2$, heating or cooling occurs at the interface. This is because the energy per carrier in the materials is different. Therefore, the amount of heat transported towards the interface is different from the heat flowing away. The principle of electronic heating and cooling is used in Peltier elements.

age scales with the difference between the temperature of the junction and a reference temperature away from the junction.

The Peltier effect The Peltier effect arises when a current I is sent through a junction of two materials with a different Seebeck coefficient. This means that the amount of energy that is carried per charge carriers is different for these two materials, as described in previous paragraph. Because the amount of charge flowing towards the junction is the same as the amount flowing away from it (conservation of charge), there will be a net accumulation of energy. The heat accumulation at the junction is then given by

$$\dot{Q} = (\Pi_1 - \Pi_2)I, \tag{3.8}$$

with $\dot{Q}$ the heat rate. Depending on the sign of the difference between both Peltier coefficents $\Pi_1 - \Pi_2$, the junction heats up or cools down. Heating or cooling of the junction also depends on the direction of I.

By applying Onsager reciprocity (equation 3.4) to equation 3.5, one can relate the Peltier coefficient to the Seebeck coefficient by the *second Thompson relation*:

$$\Pi = ST, \tag{3.9}$$

showing the close connection between the Seebeck and the Peltier effect.

3.2 Thermal and thermoelectric transport properties of graphene

Graphene is a very interesting material for new thermoelectric phenomena and at the same time, thermoelectric experiments can be used to gain new information about graphene's properties. However, in order to understand its thermoelectrics, it is useful to first start with a brief description of the thermal transport properties of graphene.

3.2.1 Thermal transport properties of graphene

In 2008, Balandin and colleagues[6] measured the thermal conductivity κ of suspended graphene to be $4840 - 5300$ W m^{-1} K^{-1}.[b] Measuring the thermal transport properties of graphene is not so straight forward as its electrical characterization, because in common experimental geometries the heat flows are not limited to the graphene flake itself and therefore difficult to control. There have been several review papers

[b] Despite graphene's 2D nature, its thermal conductivity is commonly expressed in the same dimensionality as used for 3D materials (W m^{-1} K^{-1}), using the graphite inter-plane distance of 0.34 nm as its thickness.[7]

on thermal transport in graphene,[7–9] which extensively describe different measurement methods and compare the thermal transport properties of graphene systems in different geometries with each other and with other carbon allotropes. The purpose of this section is limited to a brief introduction on the physical origins of these thermal transport properties of graphene. The mechanisms of thermal transport in graphene are different than in (bulk) metals because of two main reasons:

1. The transport is mainly mediated by phonons instead of electrons, and

2. Thermal transport in nano-sized systems behaves differently from bulk materials.

Transport by phonons The contribution of electrons to the intrinsic thermal conductivity κ_e of (suspended) graphene is temperature dependent, but is less than 1% even up to room temperature.[10] Thermal transport in graphene is thus mostly determined by the transport properties of its phonons. The phonon dispersion relation for graphene is depicted in figure 3.3(a). Graphene has two atoms per unit cell, giving rise to acoustic (A) and optical (O) phonon branches.[11] Responsible for the heat transport are the transverse and longitudinal acoustic phonon modes (TA and LA) and, additionally, the out-of-plane acoustic mode ZA, also called a *flexural phonon*.[12]

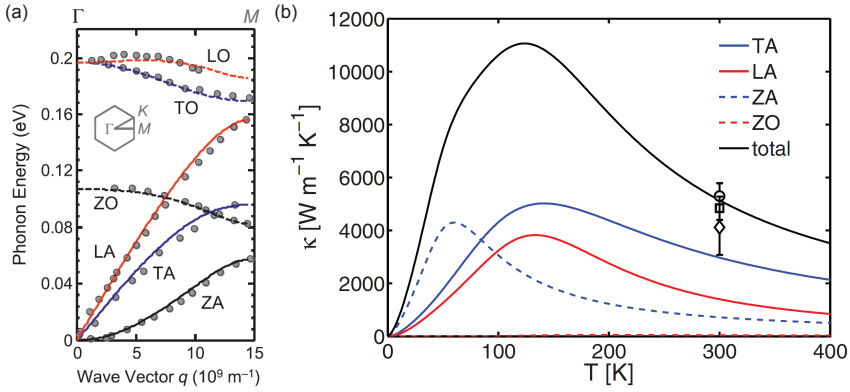

Figure 3.3: (a) Phonon dispersion (dependence of the phonon energy on its wave vector k, here q) of graphene showing the transverse (T) and longitudinal (L) branches of the optical (O) and acoustic (A) phonons. Because of its 2D nature, graphene has an extra vibrational mode out of its plane (Z). Reprinted with permission from the Materials Research Society: Reference 8. (b) Contribution to the thermal conductivity of the different phonon modes in a 5 µm wide graphene ribbon. Reprinted from Reference 13, with the permission of AIP Publishing.

For phonon dominated heat transport in 2D materials, the heat conductivity is

given by:[14]

$$\kappa = \frac{1}{2} C v_{gr} \lambda_{ph}, \tag{3.10}$$

where C is the (lattice) heat capacity per volume, v_{gr} the phonon group velocity and λ_{ph} the phonon mean free path. C has not been experimentally measured in graphene, but is usually estimated to be comparable to that of graphite $C_{graphite} \approx 1.5$ J cm^{-3} K^{-1} at room temperature. The presence of ZA phonons results in an extra contribution to the graphene heat transport, happening only at low temperature according to some studies,[8] while others claim even at room temperature.[15] The ZA mode is suppressed by the substrate for non-suspended graphene. The phonon velocity is given by $v_{gr} = \mathrm{d}\omega/\mathrm{d}k$ and is high ($\sim 10^4$ m s^{-1}),[16] a direct consequence of the steep phonon dispersion depicted in Figure 3.3(a).

The phonon mean free path λ_{ph} is also high, measured to be $\sim$ 750 nm in suspended graphene.[14] The magnitude of λ_{ph} is governed by inelastic scattering processes. [c] These processes can be divided into *extrinsic scattering* with structural imperfections such as defects, boundaries and interfaces, and *intrinsic scattering* with (quasi-)particles such as electron-phonon and Umklapp[d] scattering.[9] These are the only phonon-phonon interactions that reduce the total phonon momentum and thus shorten λ_{ph}.

Disorder coming from defects, grain boundaries, disordered edges and/or the substrate decreases the thermal conductivity of graphene from 2000–5000 W m^{-1} K^{-1} in intrinsic, suspended samples to $\sim$ 600 W m^{-1} K^{-1} in graphene on a SiO_2 substrate.[7] The lower values of κ for supported graphene is caused by enhanced extrinsic scattering due to substrate interaction.[15]

Transport in systems with lower dimensions The small size of materials like graphene has a distinct effect on κ. It can even lead to a breakdown of Fourier's law, which was for instance experimentally shown in carbon and boron nitride nanotubes.[17] When scaling down the size of a material, a number of things can happen:

1. A smaller size decreases the maximum phonon wavelength and thereby the number of available modes. This decreases the number of conduction channels and thereby the thermal conductivity.

2. Less phonon modes however, result in a lower number of available states to scatter into. Therefore the number of Umklapp processes decreases, which effectively results in an increase of the conductivity, even overcoming the first

[c] Inelastic scattering results in energy transfer from the heat carriers to their environment, thus establishing local thermal equilibrium, which is necessary for diffusive transport.

[d] An Umklapp process is the scattering of two phonons to produce a third phonon with a k-vector outside the first Brillouin zone. The first Brillouin zone is the range of k-vectors that is significant for phonon waves, as phonons with higher k are equivalent to a vector $k' = k - G$ that lies within the first Brillouin zone, with G a reciprocal lattice vector.[11]

effect.[18] In single-walled carbon nanotubes it was even reported that there is no Umklapp scattering at all.[19]

3. With smaller dimensions, scattering of the edges (especially disordered edges) becomes more important, effectively reducing the conductivity.[20]

4. For polycrystalline graphene the scattering on grain boundaries can be removed by making its typical dimensions smaller than the grain size.[21]

5. Graphene flakes smaller than λ_{ph} enter the ballistic transport regime. In this regime, κ is undefined and Fourier's law breaks down.

Thermal transfer length In the specific case of graphene on a Si/SiO_2 substrate, it is useful to have a simple picture that describes how the heat current distributes over the system after locally heating it. As depicted in figure 3.4(a), the heat flows mainly through the graphene channel because of its high κ when compared to the substrate ($\kappa_{SiO_2} \approx 1$ W m^{-1} K^{-1}). Thus a temperature gradient exists in the x-direction over a long distance in the graphene channel and in the z-direction over a very short distance into the substrate. The heat loss into the substrate results in an exponentially decaying temperature gradient along the graphene channel. The typical length over which the temperature decays is called the *thermal transfer length* L_{tt}. If we assume the Si to be a thermal reservoir at the temperature of the environment, L_{tt} is defined by:[e]

$$L_{tt} = \sqrt{\frac{\kappa_{gr} t_{gr} t_{SiO_2}}{\kappa_{SiO_2}}}, \tag{3.11}$$

with t_{gr} and t_{SiO_2} the thicknesses of the graphene and the oxide layer respectively.

This quasi-1D description of a graphene heat channel resembles the case of the spin channel from Figure 2.3, in the sense that the heat flows from a region with raised temperature (compare to a non-zero spin accumulation) towards a region with a lower, reference temperature, typically room temperature (compare with zero spin accumulation). L_{tt} is then a measure for the typical distance over which heat leaks out to the environment, analogous to λ_S, which is the typical distance over which spins relax (see section 2.1). Moreover, L_{tt} allows for an estimation of the typical thermal resistance R_T of the graphene geometry from Figure 3.4, given by

$$R_T = \frac{L_{tt}}{2\kappa_{gr} w_{gr} t_{gr}}, \tag{3.12}$$

where the factor 2 in de denominator arises from the fact that the heat can flow in both directions. Hence, the heat currents and temperature profiles in the device can

[e] The derivation of this expression is analogous to that of the transfer length in the current crowding problem, which defines the effective width of charge current injection between two materials with different resistances.[22]

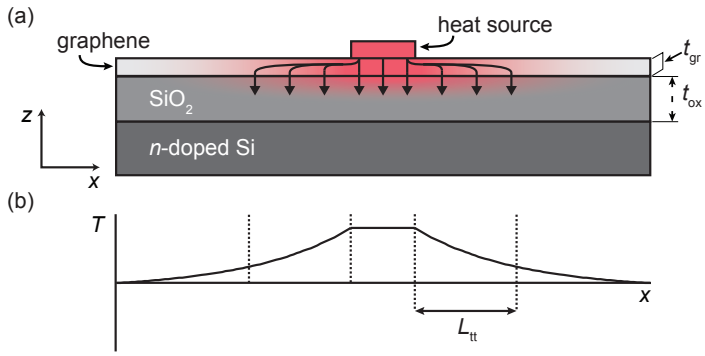

Figure 3.4: Concept of the thermal transfer length L_{tt}. (a) In the typical graphene on Si/SiO_2 geometry heat flows mostly away through the graphene, but also partly into the substrate. (b) The result is an exponentially decaying temperature profile in the graphene heat channel. The typical length scale over which the temperature drops to $1/e$ its initial value is given by L_{tt}.

be approximated by writing down the equivalent circuit, in which heat-flows into additional contacts can be represented by parallel heat resistances.

3.2.2 Thermoelectric experiments in graphene

Graphene is a special thermoelectric material, because of the strong dependence of its conductivity on energy. Therefore, its Seebeck coefficient S can be modulated by changing the Fermi energy using a back gate in a standard graphene on Si/SiO_2 field-effect transistor (FET) geometry.

Electronic measurement In 2009, Zuev and colleagues[23] experimentally determined S to be 50–100 μV K^{-1} at room temperature by using the device geometry shown in the upper inset of Figure 3.5. This scheme, first used for carbon nanotubes thermoelectrics,[24] consists of a small on-chip Au wire that acts as a heat source by sending a large current through. The resistive (Joule) heating of the heat source results in a temperature gradient in the graphene, which is then picked up by measuring the 4-probe resistance of a gold bar that is fabricated across the graphene flake. Because its resistance scales linearly with the temperature, the bar acts as a local thermometer. The gate voltage dependence of S is obtained by mapping the local temperature ΔT and the induced Seebeck voltage ΔV along the graphene flake. It has been found that S in graphene has the typical shape as shown in Figure 3.5(b), changing sign when going from the electron to the hole regime. This measurement technique is currently the most common tool to investigate graphene thermoelectric properties.

Another way of obtaining the gate dependence of S is by taking the conductivity

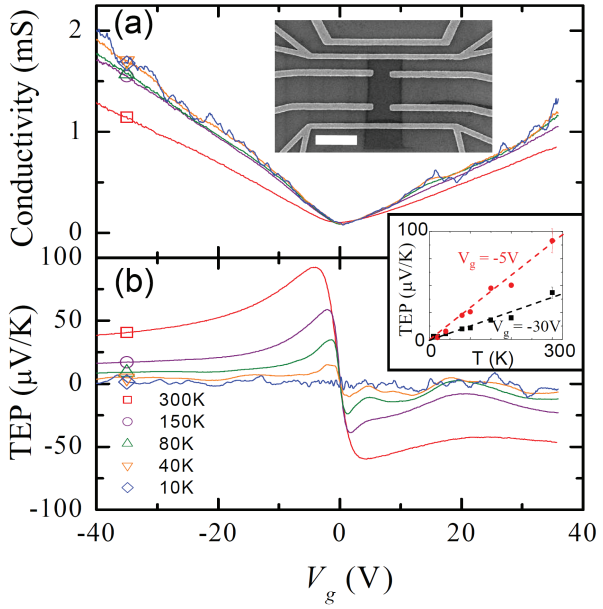

Figure 3.5: Measurement of the Seebeck coefficient of graphene (here called thermoelectric power or TEP). (a) Gate voltage dependence of the conductivity. The upper inset shows the device geometry including the graphene flake in dark gray, the heat source and two thermistors. (b) Typical shape of the gate modulated Seebeck coefficient of graphene, reversing its sign when crossing the charge neutrality point at ~ 0 V. The figure shows measurements at different temperatures, summarized in the lower inset. Reprinted with permission from Reference 23. Copyright (2009) by the American Physical Society.

measurements shown in Figure 3.5(a), and then apply the Mott relation (Eq. 3.6). This can be done by using:

$$\left.\frac{\mathrm{d}\ln\sigma(E)}{\mathrm{d}E}\right|_{E=E_\mathrm{F}} = \left.\frac{1}{\sigma}\frac{\mathrm{d}\sigma}{\mathrm{d}V_\mathrm{g}}\frac{\mathrm{d}V_\mathrm{g}}{\mathrm{d}E}\right|_{E=E_\mathrm{F}}, \tag{3.13}$$

where the back gate voltage V_g is related to the energy by:

$$\frac{\mathrm{d}V_\mathrm{g}}{\mathrm{d}E_\mathrm{F}}(V_\mathrm{g}) = \frac{\sqrt{|e|}}{\pi C_\mathrm{g}}\frac{2}{\hbar v_\mathrm{F}}\sqrt{V_\mathrm{g}-V_\mathrm{D}}. \tag{3.14}$$

Here, C_g is the gate capacitance typically in the order of ≈ 100 aF μm^{-2} and V_D the voltage at the charge neutrality point or Dirac point.

By independently measuring the energy dependence of G and of S, it becomes possible to test the validity of the Mott relation. Moreover, because thermoelectric properties are given by energy derivatives of electronic quantities, thermoelectric

measurements are most sensitive around the Fermi energy and can be used for obtaining information that is difficult or even not possible to investigate using regular (charge) transport experiments. For one, deviations from the Mott relation give information about the nature of scattering.[25] Examples are electron scattering on acoustic phonons, which should become considerable above 100 K[26] and scattering on screened charge impurities which have a quadratic dependence of S at high temperatures.[27]

It has been found that the Mott relation holds for lower temperature and away from the charge neutrality point, but deviates near the Dirac point in high mobility samples[28] as well as in bilayer graphene for low carrier densities.[9, 29] Furthermore, a quadratic dependence of S on the temperature in epitaxial graphene on SiC points to enhanced scattering on screened charge impurities.[30] In contrast, CVD-grown graphene that is transferred to SiO_2 has a linear dependence on T, which points to acoustic phonons as the dominant scattering mechanism.[31]

Atomic force microscopy based measurement Another method to investigate thermal and thermoelectric transport properties of graphene, is by using a method called *scanning Joule expansion microscopy*. This method uses an atomic force microscope to scan the topography of a simple graphene device that is covered with a thin layer of the polymer PMMA. When sending a charge current through the device, it heats up and causes the PMMA layer to expand. The mechanical expansion can then be correlated with the local temperature, making it possible to map the temperature of the device with a high temperature and spatial resolution of $\sim$ 250 mK and $\sim$ 10 nm respectively.

In reference 32 a detailed analysis was performed on the local environment of a graphene-metal contact heated by a charge current. The temperature profile was compared with a detailed simulation, making it possible to distinguish between Joule heating, current crowding effects and Peltier heating and cooling. From the Peltier contribution, identified by a switch between heating and cooling when reversing the current direction, it was possible to verify the magnitude of the Seebeck coefficient.

Applications To conclude this chapter, some remarks can be made about the significance of graphene for thermoelectric applications. One of the promises of thermoelectric materials is their use for power generation from heat. The importance of nanomaterials for the application of thermoelectric power generation started with the work of Hicks and Dresselhaus[33] in 1993. In their paper, they focused on new ways to increases the so-called thermoelectric figure of merit:

$$Z = \frac{S^2\sigma}{\kappa} \tag{3.15}$$

The quantity Z, or rather the dimensionless number ZT, is a measure for how favorable the material is in converting heat into energy. The problem of increasing normal

materials to values > 1 is the interdependence between electrical and heat conductivity (σ and κ) in many materials. Hicks and Dresselhaus introduced a new route to improve ZT by confining electrons into a 2D potential (2D quantum well). Later studies have experimentally shown that embedding thermoelectric materials into a layered superlattice indeed significantly enhances ZT.[34, 35]

The 2D-nature of graphene, its high Seebeck coefficient, and the possibility to control its thermal and electric properties, could make it a very interesting system for applications. Chemical functionalization or combining with other 2D materials in heterostructures (stacks) could help in managing local heating effects in small scale electronics. Decreasing κ of such devices would be useful for thermal insulation, but if at the same time σ can be kept at its high values, it could lead to a significant increase in ZT. Hence, further technological development of thermoelectric properties of graphene and other 2D materials, could make power generation using waste heat a feasible application.

References

[1] R. Franz and G. Wiedemann. 'Ueber die Wärme-Leitungsfähigkeit der Metalle'. *Ann. Phys.* **165**, 497 (1853).

[2] L. Lorenz. 'On the thermal and electrical conductivities of metals'. *Ann. Physik* **13**, 422 (1881).

[3] L. Onsager. 'Reciprocal Relations in Irreversible Processes. I.' *Phys. Rev.* **37**, 405 (1931).

[4] M. Cutler and N. F. Mott. 'Observation of Anderson Localization in an Electron Gas'. *Phys. Rev.* **181**, 1336 (1969).

[5] H. Fritzsche. 'A general expression for the thermoelectric power'. *Solid State Communications* **9**, 1813 (1971).

[6] A. A. Balandin, S. Ghosh, W. Bao, *et al.* 'Superior Thermal Conductivity of Single-Layer Graphene'. *Nano Lett.* **8**, 902 (2008).

[7] A. A. Balandin. 'Thermal properties of graphene and nanostructured carbon materials'. *Nat Mater* **10**, 569 (2011).

[8] E. Pop, V. Varshney, and A. K. Roy. 'Thermal properties of graphene: Fundamentals and applications'. *MRS Bulletin* **37**, 1273 (2012).

[9] Y. Xu, Z. Li, and W. Duan. 'Thermal and Thermoelectric Properties of Graphene'. *Small* **10**, 2182 (2014).

[10] S. Yiğen, V. Tayari, J. O. Island, *et al.* 'Electronic thermal conductivity measurements in intrinsic graphene'. *Phys. Rev. B* **87**, 241411 (2013).

[11] C. Kittel. *Introduction to Solid State Physics* (John Wiley & Sons) (2005).

[12] D. L. Nika and A. A. Balandin. 'Two-dimensional phonon transport in graphene'. *J. Phys.: Condens. Matter* **24**, 233203 (2012).

[13] Z. Aksamija and I. Knezevic. 'Lattice thermal conductivity of graphene nanoribbons: Anisotropy and edge roughness scattering'. *Applied Physics Letters* **98**, 141919 (2011).

[14] S. Ghosh, I. Calizo, D. Teweldebrhan, *et al.* 'Extremely high thermal conductivity of graphene: Prospects for thermal management applications in nanoelectronic circuits'. *Applied Physics Letters* **92**, 151911 (2008).

[15] J. H. Seol, I. Jo, A. L. Moore, *et al.* 'Two-Dimensional Phonon Transport in Supported Graphene'. *Science* **328**, 213 (2010).

[16] M. S. Dresselhaus and P. C. Eklund. 'Phonons in carbon nanotubes'. *Advances in Physics* **49**, 705 (2000).

[17] C. W. Chang, D. Okawa, H. Garcia, *et al.* 'Breakdown of Fourier's Law in Nanotube Thermal Conductors'. *Phys. Rev. Lett.* **101**, 075903 (2008).

[18] S. Ghosh, W. Bao, D. L. Nika, *et al.* 'Dimensional crossover of thermal transport in few-layer graphene'. *Nat Mater* **9**, 555 (2010).

[19] C. Yu, L. Shi, Z. Yao, *et al.* 'Thermal Conductance and Thermopower of an Individual Single-Wall Carbon Nanotube'. *Nano Lett.* **5**, 1842 (2005).

[20] A. D. Liao, J. Z. Wu, X. Wang, *et al.* 'Thermally Limited Current Carrying Ability of Graphene Nanoribbons'. *Phys. Rev. Lett.* **106**, 256801 (2011).

[21] D. L. Nika, S. Ghosh, E. P. Pokatilov, *et al.* 'Lattice thermal conductivity of graphene flakes: Comparison with bulk graphite'. *Applied Physics Letters* **94**, 203103 (2009).

[22] D. K. Schroder. *Semiconductor Material and Device Characterization* (John Wiley & Sons) (2006).

[23] Y. M. Zuev, W. Chang, and P. Kim. 'Thermoelectric and Magnetothermoelectric Transport Measurements of Graphene'. *Phys. Rev. Lett.* **102**, 096807 (2009).

[24] J. P. Small, K. M. Perez, and P. Kim. 'Modulation of Thermoelectric Power of Individual Carbon Nanotubes'. *Phys. Rev. Lett.* **91**, 256801 (2003).

[25] T. Löfwander and M. Fogelström. 'Impurity scattering and Mott's formula in graphene'. *Phys. Rev. B* **76**, 193401 (2007).

[26] T. Stauber, N. M. R. Peres, and F. Guinea. 'Electronic transport in graphene: A semiclassical approach including midgap states'. *Phys. Rev. B* **76**, 205423 (2007).

[27] E. H. Hwang, E. Rossi, and S. Das Sarma. 'Theory of thermopower in two-dimensional graphene'. *Phys. Rev. B* **80**, 235415 (2009).

[28] D. Wang and J. Shi. 'Effect of charged impurities on the thermoelectric power of graphene near the Dirac point'. *Phys. Rev. B* **83**, 113403 (2011).

[29] S.-G. Nam, D.-K. Ki, and H.-J. Lee. 'Thermoelectric transport of massive Dirac fermions in bilayer graphene'. *Phys. Rev. B* **82**, 245416 (2010).

[30] X. Wu, Y. Hu, M. Ruan, *et al.* 'Thermoelectric effect in high mobility single layer epitaxial graphene'. *Applied Physics Letters* **99**, 133102 (2011).

[31] A. V. Babichev, V. E. Gasumyants, and V. Y. Butko. 'Resistivity and thermopower of graphene made by chemical vapor deposition technique'. *Journal of Applied Physics* **113**, 076101 (2013).

[32] K. L. Grosse, M.-H. Bae, F. Lian, *et al.* 'Nanoscale Joule heating, Peltier cooling and current crowding at graphene-metal contacts'. *Nat Nano* **6**, 287 (2011).

[33] L. D. Hicks and M. S. Dresselhaus. 'Effect of quantum-well structures on the thermoelectric figure of merit'. *Phys. Rev. B* **47**, 12727 (1993).

[34] R. Venkatasubramanian, E. Siivola, T. Colpitts, *et al.* 'Thin-film thermoelectric devices with high room-temperature figures of merit'. *Nature* **413**, 597 (2001).

[35] K. Biswas, J. He, I. D. Blum, *et al.* 'High-performance bulk thermoelectrics with all-scale hierarchical architectures'. *Nature* **489**, 414 (2012).